Comparison of System Concepts for Traffic Monitoring with Multichannnel SAR

Martina Gabele, German Aerospace Centre (DLR), Germany
Stefan Baumgartner, DLR, Germany
Gerhard Krieger, DLR, Germany
Karl-Heinz Bethke, DLR, Germany

Abstract

This paper addresses the ground moving target indication (GMTI) performance of space-based multi-channel synthetic aperture radar (MSAR) systems as they suffer from the high speed of the radar platform leading to a wide spread clutter spectrum and compares it with the air-based case. Opposite to classical GMTI systems near future space-based SAR systems offer only few simultaneous channels and relatively low pulse repetition frequency (PRF). The influences of PRF, antenna size and number of channels on detection performance are studied. The analysis is based on a post-Doppler approach of the optimal processor since this has the advantage that in case of stationary clutter the clutter contributions can be assumed statistically independent for each Doppler cell.

1 Introduction

Traditionally GMTI has been applied to military detection and observation of few targets. A new field of GMTI is traffic monitoring. Traffic monitoring requires snapshots of huge area traffic scenes with high repeat cycle from which traffic density and travelling velocity can be determined. The Traffic Monitoring with Air- and Space-based Radar (TRAMRAD) project aims to find system concepts which are specialized to traffic monitoring [1].
The contribution of this paper is to point out the difference in detection performance of an exemplary airborne system like F-SAR, the near-future multichannel SAR system of DLR, and a similar spaceborne system, the German SAR satellite TerraSAR-X [2], and to investigate the impact of *PRF*, receiver antenna size and number of channels on detection performance. Near future SAR systems offer only few simultaneous channels (e.g. TerraSAR-X and Radarsat-2 both offer two simultaneous channels) and relatively low *PRF*. However, as is generally known [5] azimuth positioning accuracy can strongly be improved if at least three channels are available. A low-cost method to virtually increase the number of channels is aperture switching [3]. This method is going to be used for the F-SAR and as an experimental mode for TerraSAR-X. A comparison of the two systems shows that requirements concerning *PRF* are much more severe for TerraSAR-X than for the F-SAR due to the high platform velocity. Nevertheless, the weak performance especially for slowly moving targets demands for larger antenna apertures. A future multichannel SAR system offering large antenna apertures is TanDEM-X [4], a system of two TerraSAR-X satellites flying in close formation. It is shown how the second satellite improves the GMTI performance of TerraSAR-X. However the satellite formation suffers from grating lobes due to the large satellite separation. Future GMTI satellites should rather have sparse unequally spaced antenna configurations. A solution for implementation of a sparse, advantageous antenna configuration on a single SAR satellite by use of a boom and aperture switching on transmit is presented.

2 Multichannel SAR-Systems

The basic parameters of the systems our analysis refers to are given in Table 1. All systems are operated in X-band (*9.65 GHz*) and are assumed to be power compensated such that the same signal to noise ratio (*SNR*) of *0 dB* and clutter to noise ratio (*CNR*) of *10 dB* can be assumed for each received pulse independently of the number of receiver channels per pulse and target to radar distance.

System Parameters	F-SAR	TerraSAR-X	TanDEM-X	Satellite with Boom
PRF	*5 kHz*	*3–6.5 kHz*	*3-6.5 kHz*	*6 kHz*
Antenna length	*0.8 m*	*4.8 m*	*4.8 m each*	*40m*
Velocity	*90 m/s*	*7300 m/s*	*7300 m/s*	*7300 m/s*
Slant range	*4.2 km*	*700 km*	*700 km*	*700 km*

Table 1 Parameters of systems in comparison.

3 Signal and Clutter Model

For the analysis we use a post-Doppler approach of the optimal processor [5]. Hence, for stationary Gaussian clutter the clutter contributions can be assumed uncorrelated for each Doppler cell f_D. The signals $\vec{s}(u, f_D)$ may be expressed by

$$\vec{s}(u, f_D) = \vec{a}(u(m)) \cdot e^{-jm2\pi f_D / PRF},$$

whereby $e^{-jm2\pi f_D / PRF}$ describes the temporal sampling given by the index m and $\vec{a}(u(m))$ contains the two-way antenna pattern weighting and the phase shifts between the receivers due to the distance of the effective phase centres to the origin. The target signal Doppler frequency f_D depends on the velocity v_y and the direction $u_t(m)$ of the target. However there is also a corresponding clutter cell on ground, which contains the same Doppler frequency f_D as the moving target but comes from a different direction $u_{cc}(m)$. The corresponding clutter patch is sketched in Figure 1 in bright blue. There are even more ambiguous clutter patches on the ground containing the same Doppler frequency f_D but arriving from directions $u_{ac,\,i}(m)$ due to temporal subsampling and range ambiguities. Their position and their number are dependent on the *PRF*: for low *PRF* the ambiguous clutter patches are more dense in azimuth, for high *PRF* they are more dense in range. The ambiguous clutter patches are shown in dark blue.

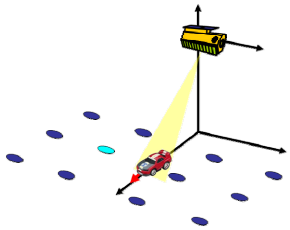

Figure 1 Moving target and corresponding (bright blue) as well as ambiguous clutter patches (dark blue).

The clutter contributions to one target Doppler frequency f_D can be modelled by the clutter contributions from the corresponding and the ambiguous clutter cells $\vec{s}(u_{ci}, f_D)$. Hence, the clutter plus noise covariance matrix C_W can be determined as follows:

$$C_W(f_D) = \sigma_N^2 I + \sum_i P_c \cdot \vec{s}(u_{c_i}, f_D) \cdot \left(\vec{s}^{\,*}(u_{c_i}, f_D) \right)^T,$$

where I is the identity matrix, σ_N^2 is the noise power, P_c the clutter power and the sum sign describes the summation over the matrices formed by the dyadic products of the sample vectors from each clutter cell. The signal to clutter and noise ratio (*SCNR*) at the output of the optimal filter can be determined by:

$$SCNR(u_t, f_D) = P_S \cdot \vec{s}(u_t, f_D) \cdot C_W^{-1}(f_D) \cdot \vec{s}^{\,*}(u_t, f_D).$$

Since the resulting detection performance is a function of the *SCNR* we use it in the following for detection performance analysis.

4 Comparison of Systems

4.1 F-SAR

As can be seen in Figure 2 the F-SAR system offers four antennas of *0.2 m* length each whereby two channels may be used for simultaneous sampling and switching between antennas is possible on transmit (ALTX) as well as on receive (ALRX). The phase centres of the transmit antennas are shown as red circles, the effective phase centres are shown as blue rhombi. The configurations to analyze are sketched in Figure 2: the single channel mode, the alternate dual channel mode (switching the receiver halves of the antenna while keeping the transmit antenna constant), the dual channel mode (simultaneous sampling by use of both receiver halves), the virtual three channel mode (switching the transmit antenna halves with simultaneous sampling with both receiver halves) and the virtual four channel mode (switching on receive between the simultaneous sampling with two quarters of the antenna and the other two quarters). Except for the three channel mode a transmit antenna of *0.2 m* length is assumed. The *PRF* is *5 kHz*, thus for the aperture switching modes the effective *PRF* reduces to *2.5 kHz*.

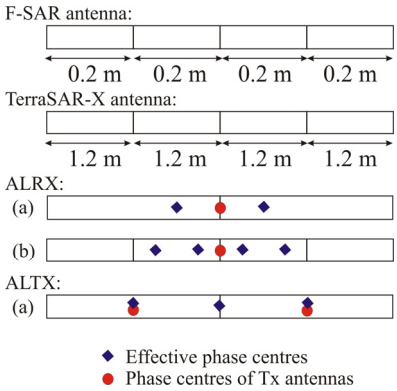

Figure 2 Effective phase centre positions obtained by ALRX and ALTX for F-SAR and TerraSAR-X.

Concerning the model shown in Figure 1 the grid size of clutter patches in azimuth is larger than the null-to-null mainbeam width for both *PRFs*. Hence, at the maximum one clutter patch in azimuth can be found in the mainbeam. Since range ambiguities can be neglected two channels are sufficient for clutter suppression and all modes with more than one receiver channel perform well. The virtual three channel mode achieves the largest maximum distance between effective phase centres and the same distance between neighbouring effective phase centres as the dual channel and the virtual dual channel mode. The four channel mode exhibits the smallest distance between neighbouring effective phase centres.

The *SCNR* curves of the multi channel modes for a snapshot of *100* temporal samples at broadside direction are shown in Figure 3 (left) dependent on the target line-of-sight (LOS) across-track velocities v_y. The

single channel mode is worst for the detection of small target velocities since in this mode a differentiation between target and clutter is possible only by use of the antenna pattern. Consequently the antenna pattern is reflected in the shape of the *SCNR* curve and for the target velocity for which the corresponding clutter cell is in the direction of the first main beam null the single channel system shows a sharp peak in performance. However, the target velocity for which the mainbeam null suppresses the corresponding clutter patch changes during the *3 dB* mainbeam integration. For high target velocities the single channel system approaches the performance of the multi channel systems. The *SCNR* curve of the three channel mode has the narrowest clutter notch since the distance of maximum phase centre separation is largest. For larger target velocities the dual channel modes as well as the three channel mode show stronger disturbances than the four channel mode because of gratinglobes resulting from the large effective phase centre separations. For long antennas and high target velocities these degradations decrease because e.g. the divided antenna mode is lower limited by the single channel mode in case of optimal processing. Since the Nyquist condition for azimuth sampling is fulfilled, the aperture switching modes perform as well as the corresponding modes with simultaneous sampling at half *PRF*.

4.2 TerraSAR-X

As was described in Figure 2 the same modes are available experimentally for the TerraSAR-X system. However for the aperture switching modes the Nyquist condition for azimuth sampling is not fulfilled. Hence, the aperture switching modes differ slightly from the corresponding modes with simultaneous sampling at half *PRF*. The *SCNR* curves of the corresponding modes with simultaneous sampling for a snapshot of *100* temporal samples at broadside direction are shown in Figure 3 (right). Due to the by far larger platform velocity the clutter notches are broader. Applying the model described in Figure 1 there is one clutter patch in azimuth within the full mainbeam if $PRF = 6\ kHz$ and two in case that $PRF = 3\ kHz$. Furthermore the aperture switching introduces a blind velocity at $v_y = \pm 47\ m/s$ due to the lowering of the effective *PRF*. Accordingly in the first case at least two channels and in the second case at least three channels are required for clutter suppression and the dual channel mode performs well while the alternating dual channel mode performs badly. The three channel mode also performs well, but the four channel mode degrades mainly because of the small distance between neighbouring effective phase centres which leads to broadening of the actual and ambiguous clutter notches.
In Figure 4 left top the *SCNR* plane of the TerraSAR-X aperture switching four channel mode over the

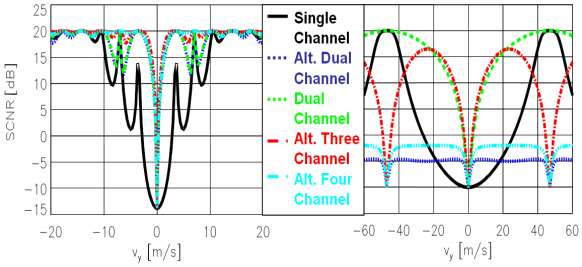

Figure 3 Comparison of *SCNR* curves for F-SAR (*PRF=5kHz*, left) and TerraSAR-X (*PRF=6kHz*, right) multichannel modes for a snapshot of *100* temporal samples at broadside direction *u=0*.

SAR integration time is approximated by dividing the coherent integration time into a consecution of subsequences of *10* pulses each and determining the *SCNR* within each subsection. As can be seen in case of temporal subsampling the performance varies during integration time while the radar is passing the grid of clutter patches. The final *SCNR* can approximately be obtained by integration along the direction *u*. There are three ways to improve the performance of the four channel mode: At first the length of the element antennas could be increased while keeping the effective phase centre separation by overlapping the antennas (Figure 4 right top). However, the effect is relatively low. Second, the effective phase centre separation could be increased (Figure 4 left bottom). This strongly improves performance. Third, the *PRF* could be increased (Figure 4 right bottom) which improves the performance by shifting the clutter patches out of the mainbeam.

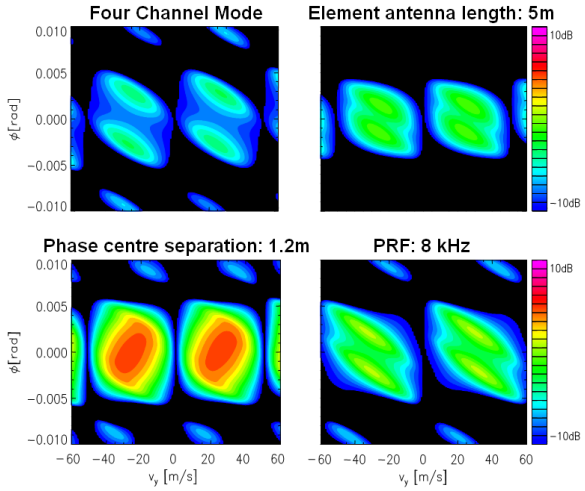

Figure 4 Performance of four channel aperture switching mode and possibilities to improve the mode.

4.3 TanDEM-X

The third system we consider is TanDEM-X. Since this system adds a second TerraSAR-X satellite to the first TerraSAR-X satellite, the system can be consid-

ered as an improvement of TerraSAR-X. This is shown in Figure 5. Analyses showed that the system performs best in case that the DPCA condition is fulfilled for each satellite. In Figure 5 both satellites are operated in dual channel mode with *PRF = 6 kHz*. The performance of the single TerraSAR-X satellite is shown in green, above in black the performance of TanDEM-X is shown. The *SCNR* curve strongly varies with target velocity. The grating lobes are introduced by the large satellite separation and lead to performance degradations down to two channel TerraSAR-X performance for certain equidistant target velocities over the whole integration time. The velocities for which performance degrades can be varied by variation of transmit frequency or satellite separation.

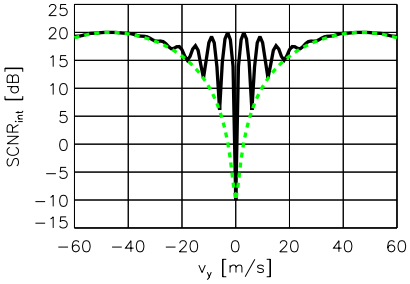

Figure 5 Comparison of *SCNR* curves for TerraSAR-X and TanDEM-X dual receive antenna mode (maximum phase centre separation: *20 m*, *PRF = 6 kHz*).

4.4 Satellite with Boom

Finally we propose a system concept which offers large antenna separations on a single satellite by use of a boom and furthermore shift the phase centres by aperture switching on transmit such that the resulting unequally spaced effective phase centre configuration yields low gratinglobes. The antenna configuration is shown in Figure 6. There are two antennas each of length *10 m* touching each other. These antennas could be placed on the satellite. The third antenna is also *10 m* long but is separated from the others by *10 m*. This could be implemented by use of a boom. If aperture switching on transmit is introduced such that transmission is switched between the leading and the trailing antenna an unequally spaced effective phase centre configuration results which effectively trades gratinglobe height against mainlobe width. The resulting *SCNR* plane is shown in Figure 7. Since the *PRF* was chosen *6 kHz*, a blind velocity occurs at $v_y = 47$ *m/s*. The blind velocity can be varied by variation of transmit frequency or *PRF*.

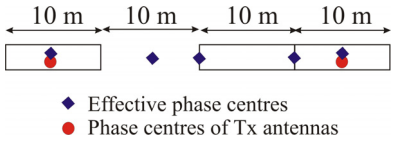

Figure 6 Satellite with Boom: Antenna configuration and effective phase centre configuration achieved by aperture switching.

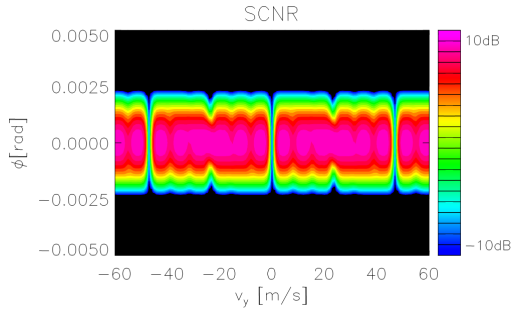

Figure 7 Low earth orbit satellite with boom (*PRF = 6 kHz*).

5 Summary

We compared the detection performance of some near future air- and spaceborne multi channel SAR systems with GMTI capability and evaluated the performance of increasing the number of spatial degrees of freedom by aperture switching and the impact of spatial and temporal subsampling. Increasing the number of channels does not necessarily improve detection performance which depends on antenna length, phase centre separation and PRF. Gratinglobes introduced by spatial subsampling result in performance degradations for certain target velocities over the whole integration time while degradations introduced by temporal subsampling vary during integration time. For assessment of the benefit of increasing the number of channels by aperture switching and in case of spatial and temporal subsampling the impact on the direction of arrival estimation accuracy should also be considered. Finally we introduced a single satellite system concept with considerably improved performance.

References

[1] Hounam, D., Baumgartner, S., Bethke, K.-H., Gabele, M., Kemptner, E., Klement, D., Krieger, G., Rode, G., Wägel, K.: *An autonomous, non-cooperative, wide-area Traffic Monitoring System using space-based Radar.* IGARSS, 2005

[2] Suess, M., Riegger, S., Pitz, W., Werninghaus, R.: *TerraSAR-X – Design and Performance*. EUSAR, 2004

[3] Lombardo, P., Colone, F.: *An Alternating Transmit Approach for STAP with Short Antenna Arrays*, IEEE, 2004

[4] Moreira, A., Krieger, G., Hajnsek, I., Hounam, D., Werner, M., Riegger, S., Settelmeyer, E.: *TanDEM-X: A TerraSAR-X Add-On Satellite for Single-Pass SAR Interferometry*. IGARSS, 2004

[5] Ender, J.H.G., Cerutti-Maori, D., Bürger, W.: *Radar antenna architectures and sampling strategies for space based moving target recognition*. IGARSS, 2005